Taylor & Francis
Taylor & Francis Group

Predictability of South American low-level jet using QuikSCAT ocean surface wind

H. WANG*†‡¶, R. FU†, J. K. SCHEMM‡, W. TANG§ and W. T. LIU§

†School of Earth and Atmospheric Sciences, Georgia Institute of Technology, Atlanta, GA 30332, USA

‡Climate Prediction Center, NCEP/NWS/NOAA, Camp Springs, MD 20746, USA

§Jet Propulsion Laboratory, California Institute of Technology, Pasadena, CA 91109, USA

¶Wyle Information Systems, McLean, VA 22102, USA

The applicability of NASA QuikSCAT ocean surface wind was tested for predicting South American low-level jets (SALLJs) with a statistical model. Our previous study (Wang, H. and Fu, R., 2004, Influence of cross-Andes flow on the South American low-level jet. *Journal of Climate*, 17, pp. 1247–1262) has examined the dynamic process associated with austral winter SALLJs using the ECMWF Reanalyses (ERA) and identified the mechanism that controls the seasonal and synoptic variations of the SALLJ. It was found that the SALLJ is maintained by strong zonal pressure gradients, with a maximum near 850 hPa caused by deflection of upstream zonal flow crossing the Andes and lee cyclogenesis. The robustness of this mechanism was further examined in this study using the NCEP–NCAR Reanalysis 1 (NCEP-R1) and NCEP–DOE Reanalysis 2 (NCEP-R2). The northerly LLJs to the east of the Andes are strongest in ERA, with wind speeds well above $15\,\mathrm{m\,s^{-1}}$. In NCEP-R1 and R2, typical wind speeds are about 12 and $10\,\mathrm{m\,s^{-1}}$, respectively. A statistical analysis of the three reanalysis datasets indicates that the SALLJ significantly correlates with the zonal wind of previous days over the South Pacific, particularly with the surface zonal wind. Based on this result, a statistical model introduced in Wang and Fu (2004) was employed in this study for forecasting the SALLJ using the QuikSCAT ocean surface wind as a predictor. The model was applied to June, July and August of 1999 to 2006 for up to 5 day forecasts of the SALLJ. Cross validations of the hindcasts indicate significant predictability of strong LLJ events with the QuikSCAT ocean surface wind data.

1. Introduction

The South American low-level jet (SALLJ) frequently occurs to the east of the Andes throughout the year, and it is strongest in austral winter (Li and Treut 1999, Nogues-Paegle *et al.* 2002). This is different from many other places, where LLJs exist only during summer (Stensrud 1996). Many studies have demonstrated that the SALLJ plays an important role in transporting water vapour from the Amazon basin to central South America and initiating convection in the La Plata River basin. Most of these analyses were carried out using the National Centers for

---

*Corresponding author. Email: hui.wang@noaa.gov

Environmental Prediction (NCEP)–National Center for Atmospheric Research (NCAR) Reanalysis 1 (NCEP-R1) data (e.g. Nogues-Paegle and Mo 1997, Berbery and Collini 2000, Marengo *et al.* 2004) and the European Centre for Medium-Range Weather Forecasts (ECMWF) Reanalysis (ERA) data (Salio *et al.* 2002, Wang and Fu 2004). However, comparisons between SALLJs in the two reanalysis datasets have not been well documented. Several recent studies have independently identified the mechanical deflection of westerly flow by the Andes as an important controlling factor of the SALLJ (Byerle and Paegle 2002, Campetella and Vera 2002, Wang and Fu 2004). Wang and Fu (2004) further developed a statistical model for forecasting SALLJ based on 700 hPa zonal winds over the subtropical eastern South Pacific. In this study, we will show that the dynamic process responsible for strong wintertime SALLJ, revealed in Wang and Fu (2004) using ERA, is also evident in NCEP-R1, as well as in the NCEP–Department of Energy (DOE) Reanalysis 2 (NCEP-R2). We will also show that the correlation of the SALLJ with the surface zonal winds of previous days over the South Pacific is higher than its correlation with the 700 hPa zonal winds. The statistical model introduced in Wang and Fu (2004) is thus applied in this study to make the SALLJ forecasts based on the surface zonal wind. However, the application of this model requires near real-time surface wind field over the South Pacific, which is not available in any reanalysis data. Ocean surface winds, measured by the SeaWinds scatterometer on the National Aeronautics and Space Administration (NASA) QuikSCAT satellite (Graf *et al.* 1998), provide a unique opportunity for the real-time implementation of this model. In addition, the statistical model used is mainly based on the dynamic processes. The forecasts made by this simple method could act as 'MOS'-type forecasts to complement those made by a numerical weather prediction model (e.g. Horel *et al.* 2002). The purpose of this study is to compare SALLJs in the three reanalysis datasets, to apply the QuikSCAT ocean surface wind to predicting the SALLJ with the statistical model and to assess the predictability of the SALLJ.

2. Data and methods

The data consist of the three-dimensional atmospheric wind field, 925 hPa temperatures and 850 hPa geopotential heights from ERA, NCEP-R1 and R2 on a 2.5° latitude × 2.5° longitude grid at 17 pressure levels. We use daily-average data over a 15 year period (1979 to 1993). The ECMWF Operational Analysis (ECOA) data from 1993 to 2002, NCEP-R1 and R2 from 1993 to 2006 and QuikSCAT ocean surface winds from 1999 to 2006 are employed for predicting the SALLJ in austral winter months, June, July and August (JJA), when the SALLJ is strongest. Although the SALLJ more effectively transports moisture from the Amazon basin feeding convection in central South America in austral summer, it is less affected by the upstream flow pattern over the South Pacific. Therefore, the predictability of the SALLJ based on the upstream zonal wind is lower in austral summer than in winter.

   Three conventional statistical techniques, including compositing, correlation and linear regression, are used. Composites, based on extremely strong LLJs, are used to characterize the circulation patterns that are associated with the SALLJ. The correlation and linear regression analyses are used in the statistical model to identify the region in the South Pacific where surface zonal wind is most closely correlated with the LLJ. The zonal wind in this region is thus used as a predictor for the direction and strength of the SALLJ based on its regression coefficients with the LLJ.

3. Comparison of the SALLJ in ERA, NCEP-R1 and R2

Since the SALLJ is oriented poleward with wind maxima near 850 hPa, we use daily 850 hPa meridional winds averaged over the LLJ region, referred to as an LLJ index hereafter, to represent the SALLJ variability. Similarly to Wang and Fu (2004), a domain of $(55°–65°\,W, 15°–25°\,S)$ is chosen for LLJ indices of austral winter, spring and autumn, and a parallelogram longitudinally bounded by $(62.5°–72.5°\,W)$ at $10°\,S$ and $(52.5°–62.5°\,W)$ at $20°\,S$ for summer, because of a significant northward shift of the LLJ during the Amazon rainy season. The 15 year (1979 to 1993) daily LLJ indices derived from the three reanalysis datasets exhibit strong daily fluctuations. The coherence of the SALLJ among these reanalysis products is examined by correlating the 15 year daily LLJ indices from different datasets for each calendar month, as shown in figure 1. The SALLJ displays similar fluctuations on a daily basis in the three datasets, with correlations greater than 0.9 between NCEP-R1 and R2 in all 12 months and greater than 0.9 between ERA and NCEP-R1/R2 in April to November. The difference in the LLJ variation between NCEP-R1 and R2 is smaller than their differences from ERA, especially during summer. Figure 1 indicates that large differences exist between ERA and NCEP-R1/R2 during the Amazon rainy season. Since the SALLJ most significantly correlates with Amazon rainfall in the summer season and also lags the monsoon circulation (Wang and Fu 2004), the large differences between ERA and NCEP-R1/R2 are presumably due to differences in rainfall pattern and associated heating among different datasets (not shown).

To compare the intensity of the SALLJ in the three reanalysis datasets, figure 2 shows the vertical-longitudinal cross sections of meridional wind composites at $15°\,S$ for January and $20°\,S$ for July, where the SALLJ has the highest frequency of occurrence. The composites are based on the top 20% of northerly wind events in the relevant LLJ indices. The months of January and July are chosen to represent austral summer and winter, respectively, since the monthly composites in figure 2 are very similar to corresponding seasonal composites. Figure 2 reveals the same major LLJ features as described in Wang and Fu (2004), with low-level maximum winds and nocturnal intensification (not shown). In general, the SALLJs are stronger in winter ($>10\,m\,s^{-1}$) than in summer ($\sim 8\,m\,s^{-1}$). The intensity of summer LLJs is comparable among the three datasets. In winter, the intensity is strongest in ERA, with maximum northerly winds of $18\,m\,s^{-1}$. The LLJs in NCEP-R1 are slightly
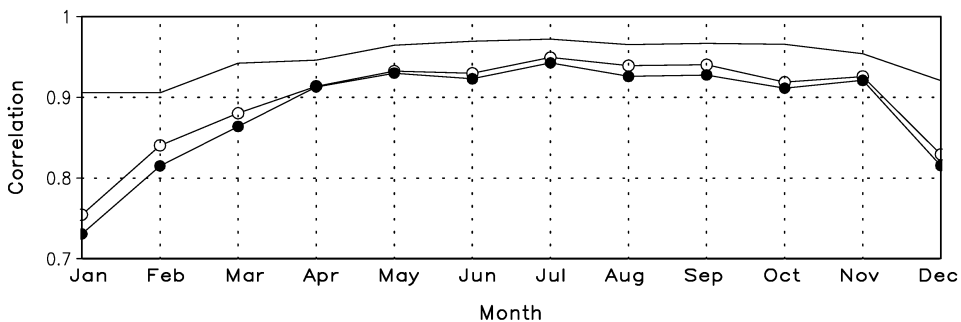

Figure 1. Correlations between 15 year (1979 to 1993) time series of daily 850 hPa meridional wind averaged over the SALLJ region (LLJ index) in ERA and NCEP-R1 (open circle), in ERA and NCEP-R2 (closed circle) and in NCEP-R1 and NCEP-R2 (no mark) for each month.
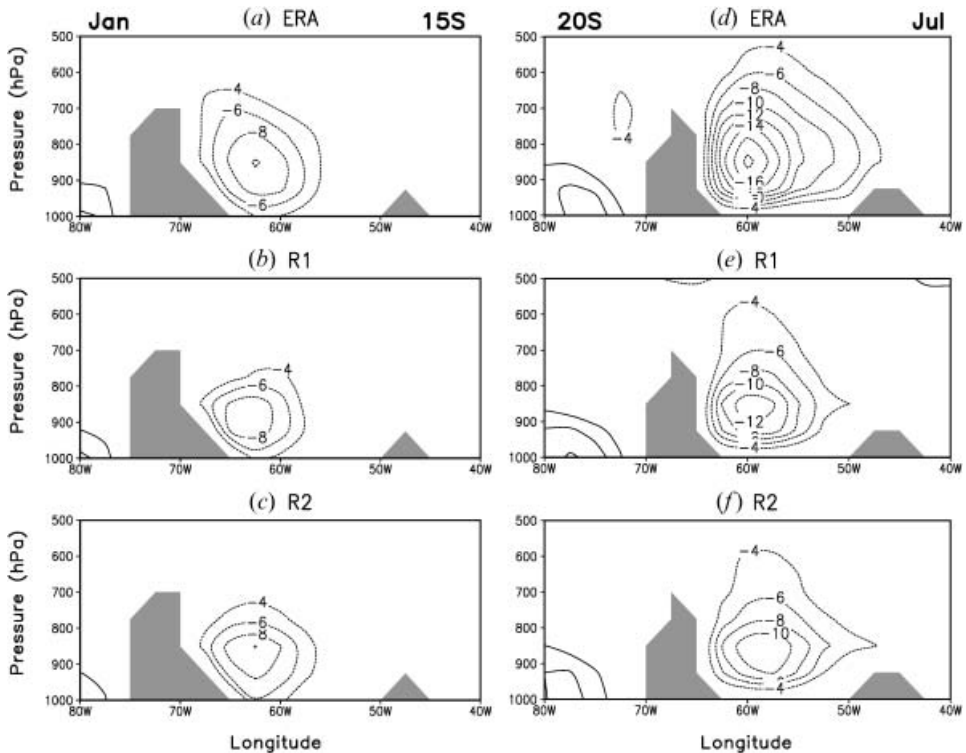
Figure 2. Composites of daily meridional wind in vertical-longitudinal cross sections at 15° S for January (left) and 20° S for July (right), based on the top 20% of northerly LLJs in the 1979 to 1993 period in (*a,d*) ERA, (*b,e*) NCEP-R1 and (*c,f*) NCEP-R2. Contour interval is 2 m s^{-1} with negative values dashed. Contours between -4 and 4 m s^{-1} are omitted. Shadings are topography.

stronger than those in NCEP-R2, with maximum wind speeds of 12 and 10 m s^{-1} in NCEP-R1 and R2, respectively. A possible explanation for the 50% difference in the LLJ intensity between ERA and NCEP-R1/R2 is the higher model resolution (T106) in the ECMWF data assimilation system (Gibson *et al*. 1997) than that (T62) in NCEP-R1/R2 (Kalnay *et al*. 1996, Kanamitsu *et al*. 2002). The terrain effect could be better resolved in ERA, leading to the stronger LLJ.

The mechanism responsible for the strong SALLJ in winter was described in Wang and Fu (2004). The SALLJ is primarily maintained by strong zonal pressure gradients to the east of the Andes through geostrophic balance. The latter are induced by a westerly flow crossing the Andes and lee cyclogenesis. The consistency of this process is now examined across three different datasets by creating a similar composite analysis of thermal and dynamic fields associated with the top 20% of northerly LLJ events. Figure 3 presents the composites of 925 hPa temperature and 850 hPa height, respectively, with 850 hPa wind for July using the three reanalysis data. In the presence of a strong northerly LLJ, no apparent zonal temperature gradient is found at 925 hPa along the east slope of the Andes in either NCEP-R1 or R2 (figures 3(*b*) and (*c*)), which is similar to that in Wang and Fu (2004) with the ERA data, as duplicated in figure 3(*a*). The strong northerly flow at 850 hPa is normal to the 925 hPa isotherms. This confirms that the SALLJ is not caused primarily by lower-level zonal temperature gradients, in contrast with LLJs

850 hPa Wind and 925 hPa Temperature
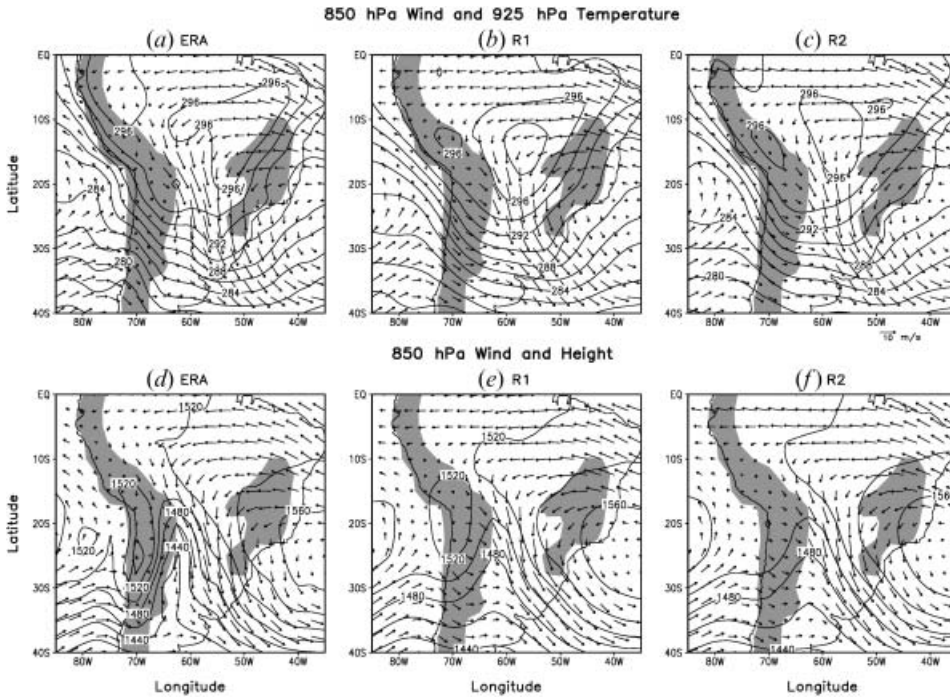

850 hPa Wind and Height

Figure 3. Composites of 925 hPa temperature (upper) and 850 hPa height (low) with 850 hPa wind (vectors), based on the top 20% of northerly LLJs in July 1979 to 1993 in (a,d) ERA, (b,e) NCEP-R1 and (c,f) NCEP-R2. Contour intervals are 2 K in (a) to (c) and 20 m in (d) to (f). Shadings indicate topography.

occurring in other places such as the Great Plains of the central United States (Bonner and Paegle 1970), the Northern Territory of Australia (Brook 1985) and the western Caribbean basin (Whyte *et al*. 2008). Consistent with Wang and Fu (2004) with ERA, the 850 hPa height field based on NCEP-R1 and R2 also displays a ridge on the upwind side of the Andes and a trough on the lee side (figures 3(*e*) and (*f*)), which is a typical flow pattern in the presence of orography (Smith 1982). The LLJs close to 60° W are nearly parallel to the height contours. The strong northerly flow is thus maintained by large zonal height gradients associated with the lee trough through geostrophic balance. The latter is closely related to westerly flow crossing a mountain, the corresponding orographically induced pressure disturbance and lee cyclogenesis (Wang and Fu 2004). The resemblance in the thermodynamic fields among the three datasets suggests that the maintenance mechanism of the SALLJ described in Wang and Fu (2004) with ERA is consistent with NCEP-R1 and R2. Weaker LLJs in NCEP-R1 and R2 (figures 2(*e*) and (*f*)) are dynamically consistent with slightly weaker zonal height gradients (figures 3(*e*) and (*f*)), as compared to those in ERA (figures 2(*d*) and 3(*d*)). Since the NCEP data assimilation system is more sensitive to the data availability than the ERA (Pawson and Fiorino 1999), this may also account for the weaker LLJ in NCEP-R1/R2 over the South American data sparse region (Herdies *et al*. 2007), in addition to the different resolutions between the two data assimilation systems.

Figure 4 presents the vertical cross sections of lag correlations at 30° S between zonal wind and the LLJ index using the three reanalysis data, respectively.
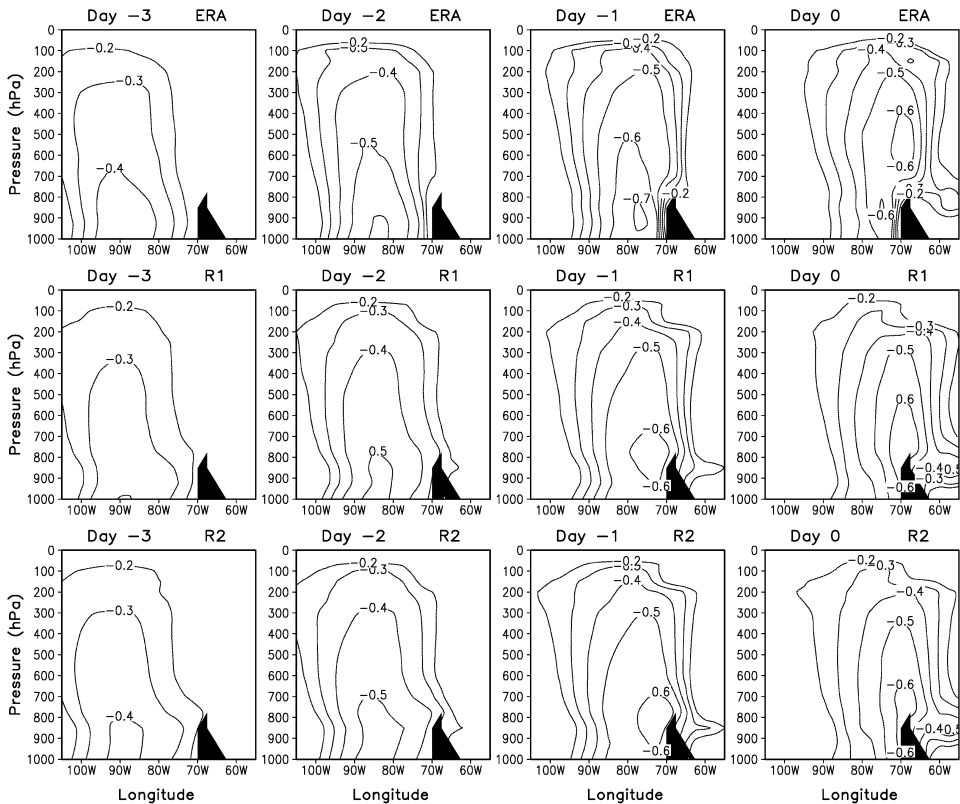
Figure 4. Correlations of zonal wind at 30° S with the LLJ index, using 15 year July daily ERA (upper panels), NCEP-R1 (middle panels) and R2 (lower panels) data. Day −2 denotes that the zonal wind leads the LLJ index by 2 days. Contour interval is 0.1. Contours between −0.2 and 0.2 are omitted. Black shadings indicate topography.

Correlation maps with NCEP-R1 (middle panels) and R2 (lower panels) are very similar to those with ERA (upper panels). The effect of upstream zonal flow on the SALLJ through 'lee troughing' is supported by the fact that the LLJ index highly correlates with the upstream zonal winds of preceding days. Significant negative correlations with the zonal wind are found throughout the troposphere over the South Pacific when the zonal wind leads the LLJ. The results are consistent with the lag correlations of 700 hPa zonal wind with the LLJ index in Wang and Fu (2004). The negative correlation indicates that the stronger the westerly flow upstream, the stronger the northerly LLJ downstream. The westerly flow over the South Pacific is actually the zonal component of lower-level cyclonic circulation associated with an upper-level trough (Wang and Fu 2004). It was suggested that the formation of the LLJ involves a low-level pressure decrease caused by both baroclinic development of the upper-level trough crossing the Andes and strong zonal winds deflected by the Andes (Wang and Fu 2004). This mechanism explains the seasonal variation of the SALLJ as described in Wang and Fu (2004). In austral summer, the mean circulation is characterized by a strong subtropical high over the South Pacific. Cyclonic disturbances associated with strong westerly flow are rare. The northerly LLJ to the east of the Andes is thus weaker in January. In winter, strong westerlies prevail in the South Pacific, which favour a strong LLJ downstream.

4. Predictability of SALLJ in ERA, NCEP-R1 and R2

Strong correlation between the LLJ index and zonal wind of preceding days (figure 4) suggests that upstream zonal wind can be used as a predictor for forecasting the SALLJ. Given an upstream zonal wind pattern over the South Pacific, the LLJ index can be predicted based on lagged relationships between the LLJ index and upstream zonal wind depicted by linear regressions, as proposed in Wang and Fu (2004). Figure 4 indicates that the correlation is higher in the lower atmosphere than in the upper atmosphere. Figure 5 shows the lag correlations of 1000 hPa zonal wind with the LLJ index in the three reanalysis datasets. Comparing to similar correlations with 700 hPa zonal wind (see figure 6 in Wang and Fu (2004)), the SALLJ is more closely related to the surface zonal wind in the South Pacific than the 700 hPa wind, particularly when the zonal wind leads the LLJ by more than 1 day. This is consistent with the physical process responsible for the SALLJ, in which the SALLJ is caused by the zonal flow deflected by the Andes, and the largest influence exerted by the Andes is on the surface flow when it crosses the mountain. Therefore, the surface zonal wind could be a better predictor for the SALLJ than the 700 hPa zonal wind used in Wang and Fu (2004). The usefulness of this forecast method and the predictability of the SALLJ based on the surface zonal wind are
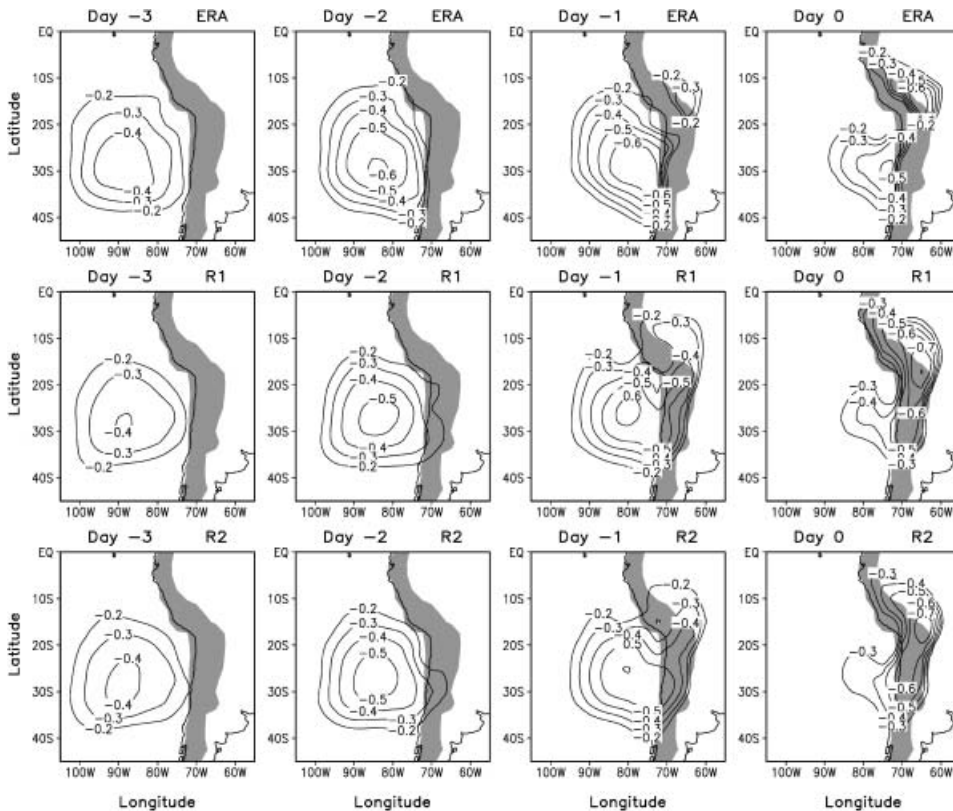

Figure 5.   Correlations of zonal wind at 1000 hPa with the LLJ index, using 15 year July daily ERA (upper panels), NCEP-R1 (middle panels) and R2 (lower panels) data. Day −2 denotes that the zonal wind leads the LLJ index by 2 days. Contour interval is 0.1. Contours between −0.2 and 0.2 are omitted. Shadings indicate topography.
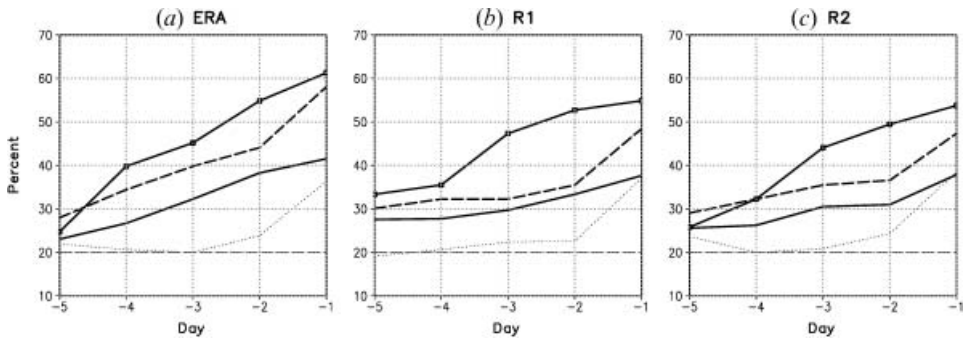
Figure 6. Percentage of hits between the LLJ index and those of hindcasts based on pure guess (thin dash), persistence (thin dot) and upstream 1000 hPa zonal wind for all five-category LLJs (thick solid), and for categories I (thick dash) and V (thick solid with open square), respectively, using 15 year (1979 to 1993) JJA data from (*a*) ERA, (*b*) NCEP-R1 and (*c*) NCEP-R2. These hindcasts are made with lead times from 5 days to 1 day.

evaluated by cross validations of daily hindcasts for 1979 to 1993 winter months (JJA), using ERA, NCEP-R1 and R2. Similarly to Wang and Fu (2004) with the 700 hPa zonal wind, we first constructed a set of 15 year (1979 to 1993) daily 1000 hPa zonal wind indices for each winter month by averaging the zonal wind in a $5°$ latitude $\times$ $5°$ longitude box over regions exhibiting highest correlations with the LLJ index (figure 5). We took both the zonal wind indices and the LLJ indices of one target month out of the data and performed a linear regression on the rest of the 14 year daily data. Hindcasts of daily LLJ index were then made for the target month using the daily 1000 hPa zonal wind index of that month and the relationship between the zonal wind index and LLJ index obtained from the linear regression. The same procedure is repeated for austral winter months (JJA) of 1979 to 1993 and for different lead times of zonal winds with respect to the LLJ. Both observed (reanalysis) and predicted LLJ indices are then evenly divided into five categories. Class I (upper 20%) represents the strongest northerly LLJs and class V (lower 20%) the strongest southerly LLJs. A hit rate used to measure the prediction skill (e.g. Wang *et al.* 1999) is the ratio of the number of hits when both the LLJ index derived from the reanalysis data and the hindcast fall into the same category to the total number of events. Figure 6 shows the hit rates for hindcasts made at different lead times from day -5 to day -1, using different reanalysis data. In all three datasets, the hit rates based on the 1000 hPa zonal wind are higher than those based on persistence and pure guess. The forecast skills are much better for extreme cases (I and V), especially in ERA (figure 6(*a*)), which are also higher than those based on the 700 hPa zonal wind (Wang and Fu 2004). The results indicate significant predictability of extreme LLJ events and the importance of upstream surface zonal wind in determining the variability of the SALLJ.

5. Forecasting SALLJ using QuikSCAT ocean surface wind

The implementation of upstream surface zonal wind in daily LLJ forecasts requires near real-time observations of surface zonal wind in the South Pacific. The ocean surface wind data collected twice daily by the NASA SeaWinds scatterometer aboard the QuikSCAT satellite provide a unique opportunity for testing the forecast model in near real-time. The QuikSCAT measurements began in July 1999 and

continue to this day, providing us with an almost continuous record of more than 7 years. To assess the applicability of the QuikSCAT winds to forecasting the SALLJ, more recent NCEP-R1 and R2 data from 1993 to 2006 are used. The ECOA data from 1993 to 2002, which have a 4 year overlap with the QuikSCAT data, are also adopted instead of the 15 year ERA data. Similar to forecasts made with 1000 hPa zonal wind in §4, the 1000 hPa zonal wind and LLJ indices from ECOA (1993 to 2002), NCEP-R1 and R2 (1993 to 2006) are used to derive the relationship between the LLJ and upstream zonal wind and the regression coefficients with the target month removed from the data. Forecasts of daily LLJ index are then made for the target month based on the QuikSCAT zonal winds of that month averaged in a $5°$ latitude $\times$ $5°$ longitude box where the zonal winds have highest correlations with the LLJ index. Similar cross validations are performed for the forecasts of JJA 1999 to 2002 with ECOA and 1999 to 2006 with NCEP-R1 and R2, as shown in figure 7. The forecast skills using the QuikSCAT data are as good as those using the 1000 hPa reanalysis zonal wind (figure 6). For certain LLJ categories and certain lead times, the forecast skills are even better with the QuikSCAT wind data. For example, the hit rate of 2 day forecasts for class V is more than 60% in ECAO (figure 7(a)) and also significantly improved for 4 and 5 day forecasts in NCEP-R1 and R2 (figures 7(b) and 7(c)). The results indicate that the QuikSCAT ocean surface wind is applicable for the near real-time forecasts of the SALLJ.

6. Conclusions

By using both NCEP-R1 and R2, we have demonstrated that the wintertime SALLJ is primarily maintained by strong zonal height gradients caused by upstream zonal flow crossing the Andes and lee cyclogenesis, consistent with the analysis with ERA in Wang and Fu (2004). It was found that the SALLJ correlates more closely with the surface zonal wind than the 700 hPa zonal winds over the South Pacific when the zonal wind leads the LLJ by more than 1 day. Therefore, the statistical model introduced in Wang and Fu (2004), which uses the 700 hPa zonal winds over the upstream South Pacific as input, was modified in this study to forecast the SALLJ using the surface zonal wind as input. A cross validation indicates significant predictability of strong LLJ events based on the surface zonal wind over the South Pacific and applicability of the QuikSCAT ocean surface wind data to real-time SALLJ forecasts. Since the SALLJ modulates much of the moisture supply and
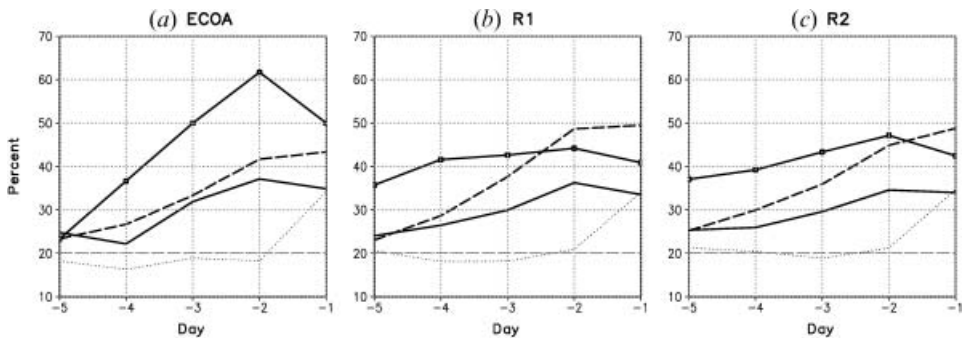

Figure 7.   As in figure 6, but using QuikSCAT ocean surface wind as a predictor for SALLJ forecasts over (a) JJA of 1999 to 2002 with ECOA, (b) JJA of 1999 to 2006 with NCEP-R1 and (c) JJA of 1999 to 2006 with NCEP-R2. Same symbols as figure 6.

rainfall in the La Plata River basin (e.g. Wang and Fu 2004), this study also indicates potential to forecast daily precipitation in this region using the same statistical model and the QuikSCAT wind data.

Acknowledgements

References

BERBERY, E.H. and COLLINI, E.A., 2000, Springtime precipitation and water vapor flux over southeastern South America. *Monthly Weather Review*, **128**, pp. 1328–1346.

BONNER, W.D. and PAEGLE, J., 1970, Diurnal variations in boundary layer winds over the south–central United States in summer. *Monthly Weather Review*, **98**, pp. 735–744.

BROOK, R.R., 1985, The Koorin nocturnal low-level jet. *Boundary-Layer Meteorology*, **32**, pp. 133–154.

BYERLE, L.A. and PAEGLE, J., 2002, Description of the seasonal cycle of low-level flows flanking the Andes and their interannual variability. *Meteorologica*, **27**, pp. 71–88.

CAMPETELLA, C.M. and VERA, C.S., 2002, The influence of Andes mountains on the South American low-level flow. In *Extended abstracts of the VAMOS/CLIVAR/WCRP conference on South American low-level jets*, 5–7 February 2002, Santa Cruz de la Sierra, Bolivia. Available online at: www-cima.at.fcen.uba.ar/sallj/index.html.

GIBSON, J.K., KALLBERG, P., UPPALA, S., NOUMURA, A., HERNANDEZ, A. and SERRANO, E., 1997, *ERA description. ECMWF Reanalysis Project Report Series: 1*. ECMWF, Reading, UK, pp. 72.

GRAF, J., SASAKI, C., WINN, C., LIU, W.T., TASI, W., FREILICH, M. and LONG, D., 1998, NASA scatterometer experiment. *Acta Astronautica*, **43**, pp. 397–407.

HERDIES, D.L., KOUSKY, V.E. and EBISUZAKI, W., 2007, The impact of high-resolution SALLJEX data on global NCEP analyses. *Journal of Climate*, **20**, pp. 5765–5783.

HOREL, J., POTTER, T., DUNN, L., STEENBURGH, W.J., EUBANK, M., SPLITT, M. and ONTON, D.J., 2002, Weather support for the 2002 Winter Olympic and Paralympic Games. *Bulletin of the American Meteorological Society*, **83**, pp. 227–240.

KALNAY, E., KANAMLTSU, M., KISTLER, R., COLLINS, W., DEAVEN, D., GANDLN, L., IREDELL, M., SAHA, S., WHITE, G., WOOLLEN, J., ZHU, Y., CHELLIAH, M., EBISUZAKI, W., HIGGINS, W., JANOWIAK, J., MO, K.C., ROPELEWSKI, C., WANG, J., LEETMAA, A., REYNOLDS, R., JENNE, R. and JOSEPH, D., 1996, The NCEP/NCAR 40-year reanalysis project. *Bulletin of the American Meteorological Society*, **77**, pp. 437–471.

KANAMITSU, M., EBISUZAKI, W., WOOLLEN, J., YANG, S.-K., HNILO, J.J., FIORINO, M. and POTTER, G.L., 2002, NCEP–DOE AMIP-II reanalysis (R-2). *Bulletin of the American Meteorological Society*, **83**, pp. 1631–1643.

LI, Z.X. and TREUT, H.L., 1999, Transient behavior of the meridional moisture transport across South America and its relation to atmospheric circulation patterns. *Geophysical Research Letters*, **26**, pp. 1409–1412.

MARENGO, J.A., SOARES, W.R., SAULO, C. and NICOLONIBO, M., 2004, Climatology of the low-level jet east of the Andes as derived from NCEP–NCAR reanalysis: characteristics and temporal variability. *Journal of Climate*, **17**, pp. 2261–2280.

NOGUES-PAEGLE, J., MECHOSO, C.R., FU, R., BERBERY, E.H., CHAO, W.C., CHEN, T.-C., COOK, K., DIAZ, A.F., ENFIELD, D.B., FERREIRA, R., GRIMM, A.M., KOUSKY, V., LIEBMANN, B., MARENGO, J., MO, K.C., NEELIN, J.D., PAEGLE, J., ROBERTSON, A.W., SETH, A., VERA, C.S. and ZHOU, J., 2002, Progress in Pan American CLIVAR research: understanding the South American monsoon. *Meteorologica*, **27**, pp. 1–30.

Nogues-Paegle, J. and Mo, K.C., 1997, Alternating wet and dry conditions over South America during summer. *Monthly Weather Review*, **125**, pp. 279–291.

Pawson, S. and Fiorino, M., 1999, A comparison of reanalyses in the tropical stratosphere. Part 3: inclusion of the pre-satellite data era. *Climate Dynamics*, **15**, pp. 241–250.

Salio, P., Nicolini, M. and Saulo, C., 2002, Chaco low-level jet events characteriztion during the austral summer season. *Journal of Geophysical Ressarch*, **107**, p. 4816.

Smith, R.B., 1982, Synoptic observations and theory of orographically disturbed wind and pressure. *Journal of the Atmospheric Sciences*, **39**, pp. 60–70.

Stensrud, D.J., 1996, Importance of low-level jets to climate: a review. *Journal of Climate*, **9**, pp. 1698–1711.

Wang, H. and Fu, R., 2004, Influence of cross-Andes flow on the South American low-level jet. *Journal of Climate*, **17**, pp. 1247–1262.

Wang, H., Ting, M. and Ji, M., 1999, Prediction of seasonal mean United States precipitation based on El Niño sea surface temperatures. *Geophysical Research Letters*, **26**, pp. 1341–1344.

Whyte, F.S., Taylor, M.A., Stephenson, T.S. and Campbell, J.D., 2008, Features of the Caribbean low level jet. *International Journal of Climatology*, **28**, pp. 119–128.